

# How cracks modify permeability and introduce velocity dispersion: Examples of glass and basalt

YVES GUÉGUEN, MATHILDE ADELINET, AUDREY OUGIER-SIMONIN, JÉRÔME FORTIN, and ALEXANDRE SCHUBNEL, *Ecole Normale Supérieure*

The porosity of igneous rocks is usually very small, although for some basalts it can be nonnegligible due to gas exsolution. In the case of glass, it is vanishingly small. Why is it of any interest to look at this kind of material from the point of view of rock physics? Two series of reasons indeed motivate such investigations.

The first one is that there is an interest to investigate basalts and glass for themselves. Basalts are an important component of the oceanic crust. Some projects consider that they could serve as storage, in particular for CCS (carbon capture and storage). Possible monitoring through seismic methods demands a sufficiently good understanding of the elastic properties. Glass is used for nuclear waste storage. In France, vitrified nuclear radioactive waste should be stored at around 400 m depth in shales. In both cases, permeability is a key parameter. Its variation with pressure in particular has to be known.

As shown in this article, basalt and glass can provide as well some insight into fundamental processes that could take place in other rocks. This is the second reason why their investigation is of great interest. Laboratory investigation of a fresh Icelandic basalt has provided a nice example of a porous-cracked rock in which frequency-dependent elastic behavior has been measured. Cracks are known to play a key role in the frequency-dependence of elastic-wave speeds. Laboratory investigation of synthetic glass in which thermal cracks were introduced in a controlled way allowed us to measure crack-induced permeability and its variation with pressure. Glass has been known for a long time to be an almost ideally elastic-brittle solid. Pioneer work of Griffith on glass around 1920 led to what became fracture mechanics.

## Dispersion of elastic moduli: Squirt flow in basalt

When cracks and pores are connected within a rock, stress can induce fluid flow from one inclusion to another one. Because cracks are more compliant than equant pores, a stress-wave builds up a higher fluid pressure within a crack than within a pore, and consequently fluid flows from crack to pore at a local scale (O'Connell and Budiansky, 1974). At low frequencies, fluid pressure has time to reach equilibrium. The elastic moduli are in that case relaxed moduli, those moduli defined within the framework of poroelastic theory (drained or undrained moduli). Such a situation can be expected at seismic frequencies. However, in laboratory conditions, most elastic-wave data are obtained in the MHz range. Clearly, in such a high-frequency range, there is no time for fluid-pressure equilibrium to take place (even at a local scale). The elastic moduli are unrelaxed moduli in that case. They are not those accounted for by poroelasticity, but they may be calculated from effective medium theory (Le Ravalec and Guéguen, 1996).

A block of basalt extracted on a road outcrop in the Reyk-

janes Peninsula has provided the sample for the experimental investigation described in the following. The sample is an alkali, fresh and young (less than 10,000 years) basalt with a connected porosity of about 8%. The pore distribution is bimodal, a fact that is of particular interest as explained below. Crack porosity is 1%, and equant pores porosity is 7%. Permeability is  $10^{-15}$  m<sup>2</sup>. Bulk modulus has been measured on water-saturated samples and on dry samples at low (0.01 Hz) and high (1 MHz) frequencies. At low frequencies, the measurement is obtained by small oscillations (less than 1 MPa) of the confining pressure. At high frequencies, the time of flight of a pulse is measured, so that the P- and S-wave velocities are obtained and provide the moduli. The experiments (Adelinet et al., 2010) have been carried out on jacketed samples (cylinders of 80 mm height by 40 mm diameter) at a constant pore pressure  $p = 10$  MPa, and at room temperature. The confining pressure was variable from  $P = 20$  up to  $P = 200$  MPa.

The results (Figure 1) show that there is a significant difference between the low-frequency, undrained, bulk modulus and the high-frequency saturated bulk modulus. The first one is expected to be the appropriate modulus for sufficiently low-frequency elastic waves (frequency range of seismology to seismics). The second one is an unrelaxed modulus that can be measured in the MHz range. From Figure 1, it is clear that the difference between both moduli decreases when pressure increases. Beyond 150 MPa, this difference becomes too small to be detected. Independent measurements show that this pressure evolution corresponds to crack closure (Figure 2). Indeed porosity, derived from strain data, decreases by about 1% from  $P = 0$  to  $P = 200$  MPa. This is in agreement with the P- and S-wave velocity variations. It is expected that crack closure should result in an increase in elastic-wave velocity. This is exactly what is observed on Figure 2. The overall conclusion is that crack closure wipes out the dispersion effect. It is thus inferred that the dispersion effect is due to the existence of cracks.

This idea leads to a simple quantitative model for calculating high- and low-frequencies moduli in a bimodal porous rock (Adelinet et al., 2011). Effective medium theory provides a way to derive unrelaxed (i.e., high-frequency) moduli for both dry and saturated porous rocks. Assuming equant pores to be spherical, and cracks to be spheroidal with an aspect ratio  $\xi = w/c$  (where  $w$  is the minor and  $c$  is the major length of the spheroid semi-axes), exact relations are known to express effective moduli, within the framework of the non-interaction approximation. Combining these results with the Biot-Gassmann equation provides furthermore the relaxed undrained modulus. Let us define modulus  $M$  (saturated) dispersion as the quantity  $D = (M_{lf} - M_{hp})/M_{hp}$ ; then  $D$  is directly obtained from the above theoretical results. In the present case of a bimodal porosity, the crack fraction  $R$  is the con-

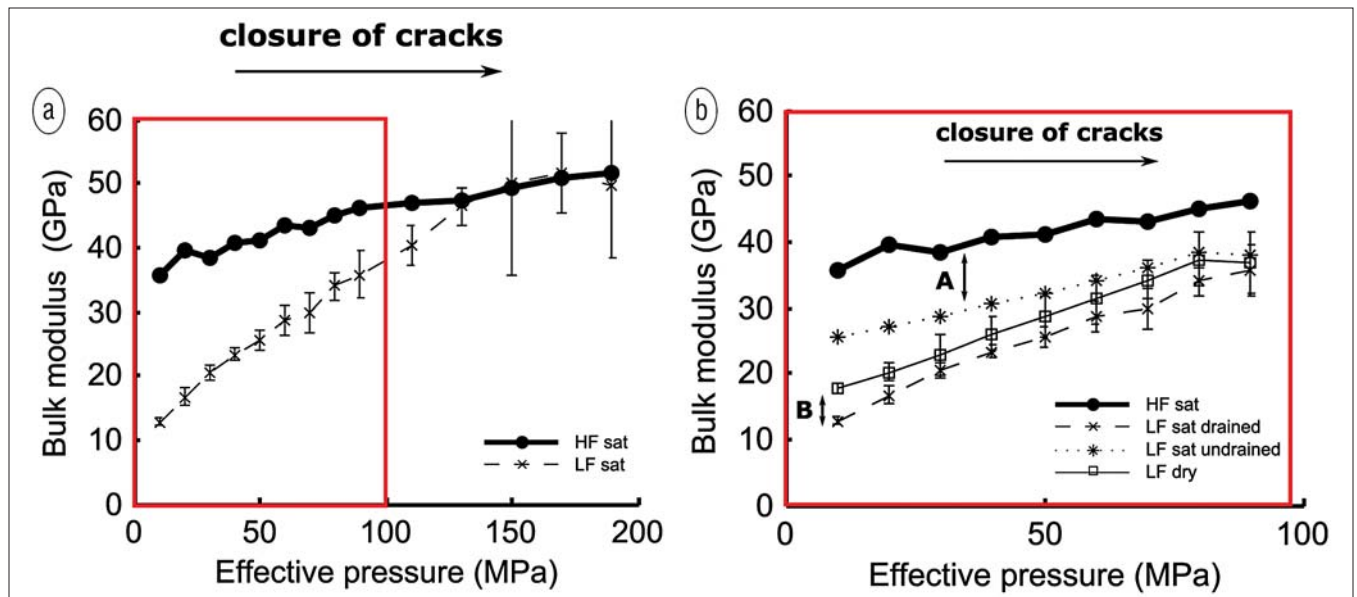


**Figure 1.** Bulk modulus obtained from high-frequency (HF) velocity inversion and low-frequency (LF) oscillation tests (Icelandic basalt); sat = saturated conditions. (a) All experimental results over the 0–190 MPa range. (b) HF, LF saturated (drained and undrained) and dry moduli over the 0–100 MPa interval. Two effects are highlighted: A (frequency effect), and B (small physico-chemical effect). (From Adelinet et al., 2010.)

Reference	Rock type (Low porosity rocks)	P* (mpa)
Yale (1984)	Tight sandstones	15.9–26.3
Brace et al. (1968)	Westerly granite	30.6
Bernabe (1986)	Chelmsford granite	34.6
	Barre granite	42.7
Fisher and Paterson (1992)	Carrara marble	21.3
Huenges and Will (1989)	Urach gneiss	20.4
Morrow et al. (1994)	Gneiss [Kola]	31.2
	Basalt [Kola]	9.8
	Amphibolite [KTB]	9.1–17.2

**Table 1.** Critical Pressure P\* for tight rocks permeability, compiled in David et al., 1994.

trolling parameter. R is defined as  $R = \Phi_{cr} / \Phi$  where  $\Phi_{cr}$  is the crack porosity, and  $\Phi$  the total porosity. Figures 3 and 4 show how  $D_k$  is predicted to vary with R for different crack aspect ratio values. Bulk dispersion  $D_k$  (Figure 3a) is predicted to be zero if there is no crack, and zero also if there are only cracks. The maximum value of  $D_k$  depends on aspect ratio. It can be as high as 30% for  $\xi = 0.01$ . The maximum is calculated to occur near  $R = 0.2$ , a value close to the precise value of the reported case. Shear dispersion  $D_G$  (Figure 3b) has no maximum; it is an increasing function of R. Our experiments, however, do not give any information on shear dispersion, so that this last prediction cannot be checked. What can be done is to check the bulk dispersion data against theoretical predictions. There is only one free parameter which is the crack aspect ratio. Figure 4 shows how theoretical predictions and experimental data can be compared, and which aspect ratio

range is compatible with the data. The conclusion is that the aspect ratio should be close to 0.01. This agrees nicely with independent results derived from elastic-wave velocity data (Figure 2).

**Crack permeability in glass**

If a connected crack network exists in a rock at large scale, it may control the rock permeability. Previously published data (David et al., 1994) show that, for low-porosity rocks, permeability decreases exponentially with increasing effective pressure. The high sensitivity of permeability to pressure is, in that case, attributed to crack closure. The pressure sensitivity is quantified through a critical pressure P\* such that  $k = k_0 e^{-(P/P^*)}$ . The value of P\* ranges approximately from 10 to 40 MPa for rocks as diverse as basalts, tight sandstones, or granites. Such a high pressure sensitivity is at contrast with the behavior of higher-porosity rocks, where equant pores are much less compliant than cracks. The consequences of this may be important for fault mechanics, and in many geotechnical issues.

Synthetic borosilicate glass samples (representative of an almost ideal isotropic brittle elastic solid) have been investigated with various crack contents (Ougier-Simonin et al., 2011a). The intact original samples were produced in conditions of slow cooling that prevents any crack formation. Then cracks have been introduced by quenching samples heated up to 300°C. Cylindrical samples (80 mm height by 40 mm diameter) were quenched in less than 5 s into distilled water at 20°C. The thermal shock produced by quenching induced a maximum tensional stress tangential to the cylinder (and perpendicular to the cylinder axis), within an outward ring.

It is thus expected that cracks should develop mainly along the vertical direction, and that crack density should decrease from the sample boundary towards the cylinder axis. In order

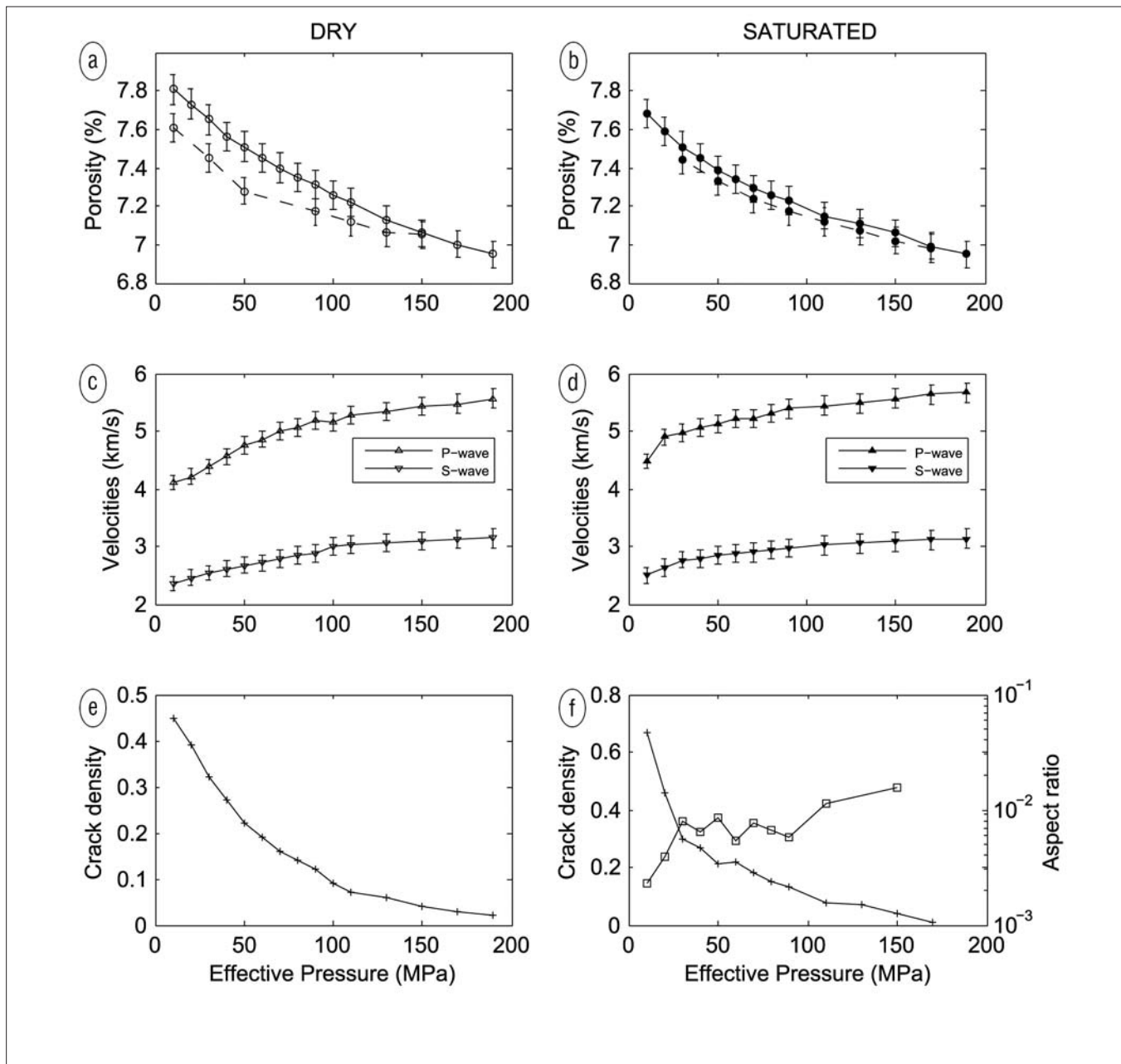


**Figure 2.** Mechanical data (porosity decrease), elastic-wave velocities, and effective medium inversion data for the triaxial experiment performed on the investigated basalt. The data are obtained in (left) dry and (right) saturated conditions, respectively. (a–b) Porosity evolution, where unloading is indicated as a dashed line. (c–d) P- and S-wave velocities (HF). (e–f) Inverted parameters from the effective medium model used by Fortin et al. (2007): crack density in dry and saturated conditions, aspect ratio in saturated conditions. (From Adelinet et al., 2010.)

to take this fact into account, we consider that the measured crack density  $\rho_c$ , obtained from elastic-wave velocities, is an apparent one (averaged over the radial section) which remains highly representative of the total crack density induced. P- and S-wave velocities are shown on Figure 5 for both intact and cracked glasses (dry, argon-saturated, and water-saturated). Velocities increase with pressure, as expected from crack closure. Inverting for crack density gives a scalar crack density  $\rho_c = 0.23$  in the dry case at zero pressure. Closure pressure is close to 20 MPa, a value that implies a crack aspect ratio  $\xi$  around  $5 \cdot 10^{-4}$ . Crack density becomes very small at pressures above 20 MPa. At these pressures, cracked glass velocities are

close to the values of the intact glass although a small difference remains.

Measurements of permeability have been achieved on samples thermally treated at 300°C in the axial direction using argon and water, through the flow and/or the pulse methods (Ougier-Simonin et al., 2011b). As discussed above, we have assumed a homogeneous distribution. The consequence is that the measured axial permeability is an apparent permeability. Pore pressure  $p$  was fixed at 5 MPa, and effective pressure (defined as  $P-p$ ) varied from 2 to 20 MPa. Higher permeability values have been measured using the flow method ( $10^{-17} - 10^{-19} \text{ m}^2$  range), lower values ( $10^{-19} - 10^{-21} \text{ m}^2$  range)

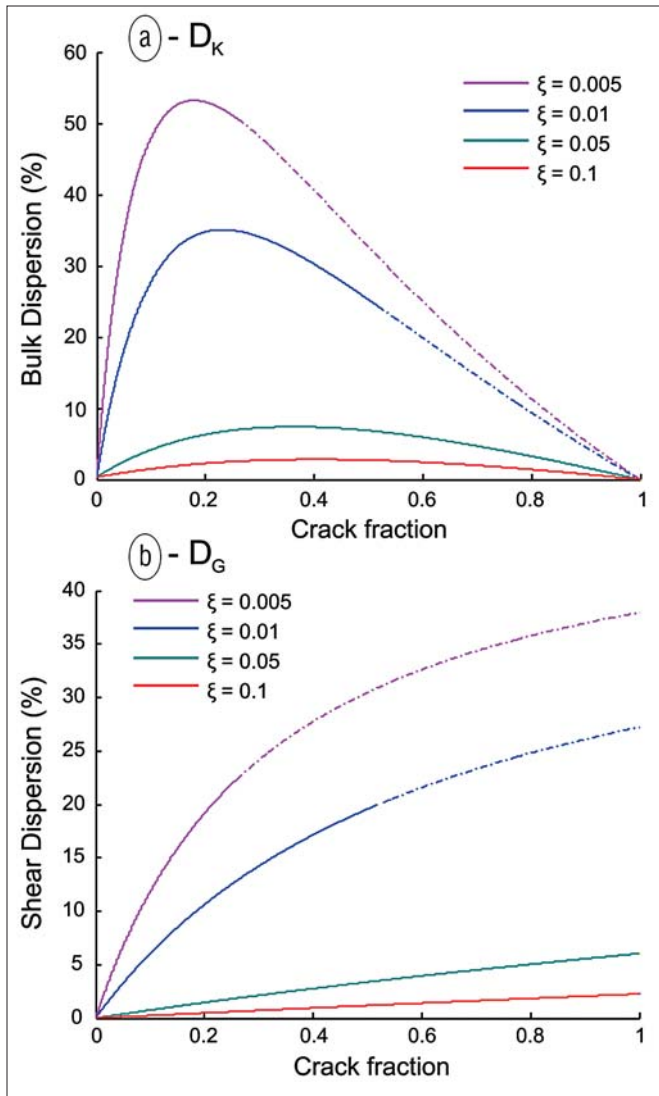


**Figure 3.** Numerical results obtained from a crack and pore effective medium model. (a) Predicted bulk dispersion  $D_K$ : dispersion increases when aspect ratio decreases. Bulk dispersion is zero when only cracks, or only pores, are present. (b) Predicted shear dispersion  $D_G$ : dispersion increases when aspect ratio decreases. Shear dispersion increases with crack fraction. (From Adelinet et al., 2011.)

have been measured using the pulse method. Permeability decreases according to the exponential law  $k = k_0 e^{-(P/P^*)}$ , where  $P^*$ , as given by the inverse of the slope, is 2.3 MPa. As shown by Figure 6, water and argon data are almost identical. Hydrostatic loading and unloading paths provide close values.

The effect of mechanical damage on permeability is to increase it. This is shown on Figure 7. Cracking induced by the deviatoric stress is visible from the P-wave velocity drop. But as crack density increases by a factor of 10, the permeability increase is more than a factor of 100. This result shows that increasing deviatoric stress, and so mechanical damage, results first in increasing crack aperture, then in increasing crack density.

These results suggest that reversible crack closure is the controlling mechanism. For a connected crack network, permeability is expected to depend on crack density  $\rho_c$ , crack aspect ratio  $\xi$ , and crack semi-aperture  $w$ ,  $k \sim \rho_c \xi w^2$ , so that

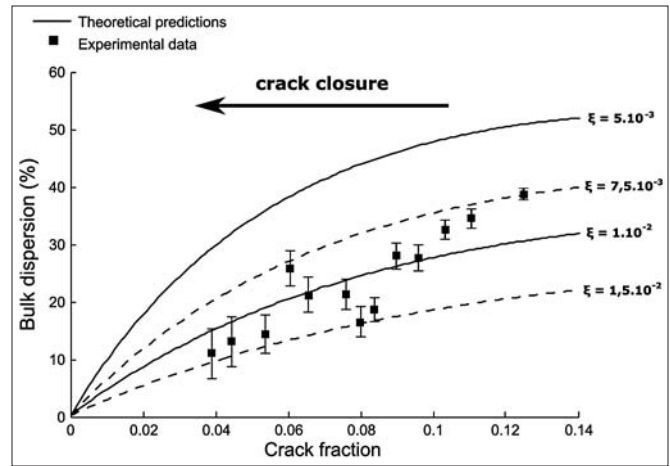


**Figure 4.** Comparison between experimental data and theoretical predictions for bulk dispersion in a cracked porous rock. Aspect ratios  $\xi$  are indicated. The experimental data are from Figures 1 and 2. It is assumed that equant porosity is constant and crack porosity only varies with pressure. (From Adelinet et al., 2011.)

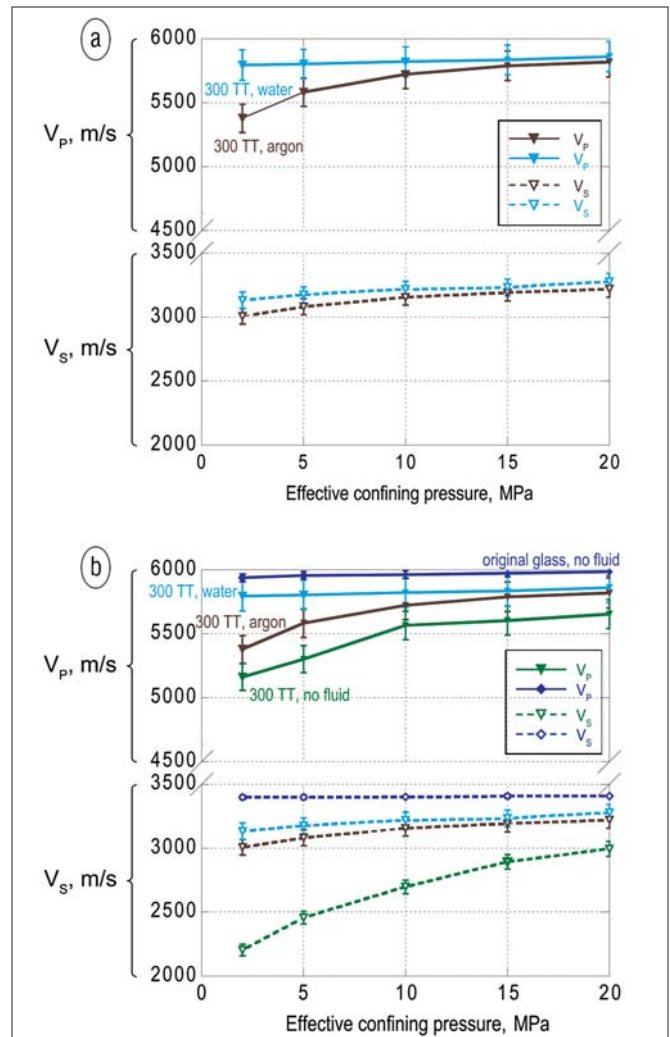


**Figure 5.** Elastic-wave velocities (P- and S-waves) in synthetic glass as a function of hydrostatic pressure. (a) Thermally cracked glass (shock at 300°C), saturated with water or argon. (b) Comparison of the previous data with the dry case (shock at 300°C) and the intact original glass (From Ougier-Simonin et al., 2011b.)

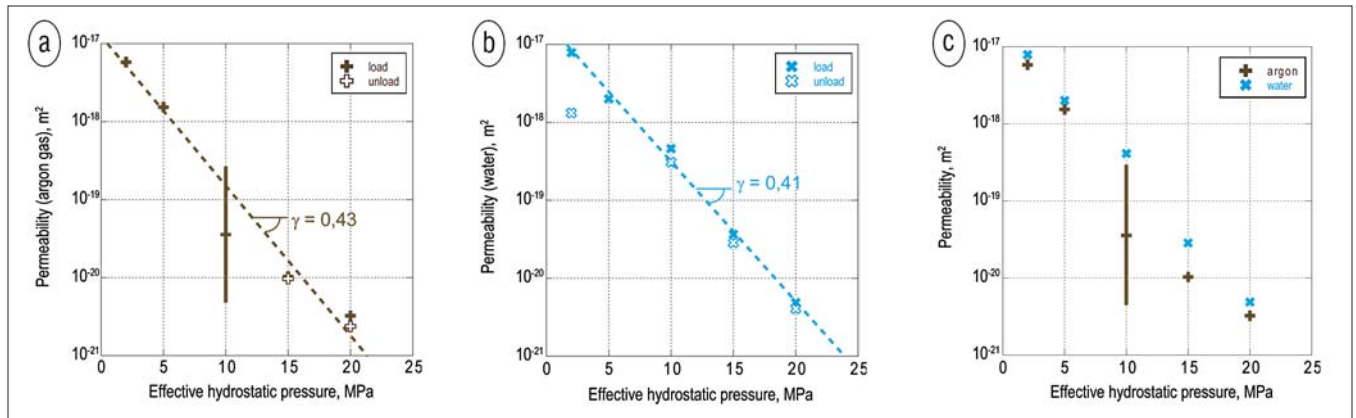


**Figure 6.** Permeability measurements in thermally cracked glass (shock at 300°C) in hydrostatic conditions. (a) Permeability data in loading and unloading conditions for argon-saturated sample. (b) Permeability data in loading and unloading conditions for water-saturated sample. (c) Comparison of argon gas and water tests in loading conditions. (From Ougier-Simonin et al., 2011b.)

at 5 MPa effective pressure,  $w$  is found to be in the range of 0.1–0.5  $\mu\text{m}$  if  $\xi$  is in the range  $10^{-4} - 10^{-3}$ , a range that is also independently expected from velocity data. Note that the  $P^*$  values are lower than those previously reported for rocks (Table 1) and compiled in David et al. (1994). Assuming that  $P^*$  is mainly reflecting the crack closure process, this means that crack closure is easier and, correlatively, that crack aspect ratio  $\xi$  is smaller than for other rocks. In other words, cracks are smoother and sharper. Indeed, it is well known that cracks are sharp in glass, a fact that reflects the nonexistence of a

microstructure. Being amorphous (a kind of frozen liquid), glass does not have any microstructure, but a nanostructure. This permeability reversibility has also been observed in basalt, which has a variable content in glassy material. For softer rocks such as clay sandstones, creep may lead to irreversible crack deformation.

### Conclusions

The existence of cracks in a porous rock may be a potential cause of large elastic-wave velocity dispersion. Although

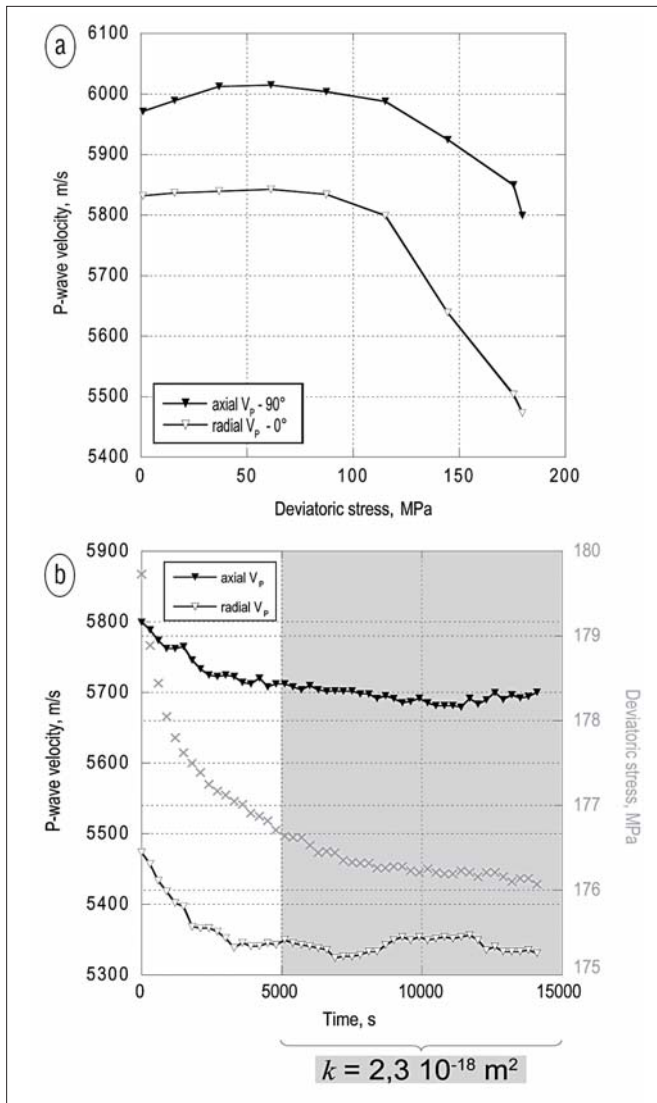


**Figure 7.** Permeability of thermally cracked glass (shock at 300°C) for argon-saturated sample under deviatoric stress. (a) Axial and radial P-wave velocity evolution during loading up to an axial stress of 200 MPa. (b) Relaxations of P- and S-waves and axial stress during the permeability measurement at high deviatoric stress. (From Ougier-Simonin et al., 2011b).

they represent a small fraction of total porosity, cracks can produce a strong dispersion due to squirt-flow processes. Experimental results on basalt submitted to high confining pressure have provided data that can be well explained by this model. Such an effect has to be accounted for when laboratory, high-frequency, data are compared to seismic or seismological data. Cracks modify also the permeability. A small crack porosity can result in a nonnegligible permeability. Furthermore, when a connected crack network is present, rock permeability is strongly pressure-sensitive. An almost ideal case has been experimentally investigated, that of glass containing a small crack porosity. Because glass has only a nanostructure, cracks are smooth and sharp in that case and pressure sensitivity very high. **TLE**

**References**

Adelinet, M., J. Fortin, Y. Guéguen, A. Schubnel, and L. Geoffroy, 2010, Frequency and fluid effects on elastic properties of basalt: Experimental investigations: *Geophysical Research Letters*, **37**, no. 2, L02303, doi:10.1029/2009GL041660.

Adelinet, M., J. Fortin, and Y. Guéguen, 2011, Dispersion of elastic moduli in a porous-cracked rock: Theoretical predictions for squirt flow: *Tectonophysics*, **503**, no. 1/2, 173–181, doi:10.1016/j.tecto.2010.10.012.

David, C., T. F. Wong, W. Zhu, and J. Zhang, 1994, Laboratory measurement of compaction-induced permeability change in porous rocks: Implications for the generation and maintenance of pore pressure excess in the crust: *Pure and Applied Geophysics*, **143**, nos. 1/2/3, 425–456.

Fortin, J., Y. Guéguen, and A. Schubnel, 2007, Effect of pore collapse and grain crushing on ultrasonic velocities and  $V_p/V_s$ : *Journal of Geophysical Research*, **112**, B08207, doi:10.1029/2005JB004005.

Le Ravalec, M. and Y. Guéguen, 1996, High and low frequency elastic moduli for a saturated porous/cracked rock (differential self-consistent and poroelastic theories): *Geophysics*, **61**, no. 4, 1080–1094, doi:10.1190/1.1444029.

O’Connell, R. J. and B. Budiansky, 1974, Seismic velocities in dry and saturated cracked solids: *Journal of Geophysical Research*, **79**, no. 35, 5412–5426, doi:10.1029/JB079i035p05412.

Ougier-Simonin, A., J. Fortin, Y. Guéguen, A. Schubnel, and F. Bouyer, 2011a, Cracks in glass under triaxial conditions: *International Journal of Science and Engineering*, **49**, no. 1, 105–121, doi:10.1016/j.ijengsci.2010.06.026.

Ougier-Simonin, A., Y. Guéguen, J. Fortin, A. Schubnel, and F. Bouyer, 2011b, Permeability and elastic properties of cracked glass under pressure: *Journal of Geophysical Research*, **116**, B7, B07203, doi:10.1029/2010JB008077.

*Acknowledgments:* This work has been supported by the CEA, the CNRS, and Ecole Normale Supérieure.

*Corresponding author:* yves.gueguen@ens.fr